SUPPLEMENTAL FIGURES

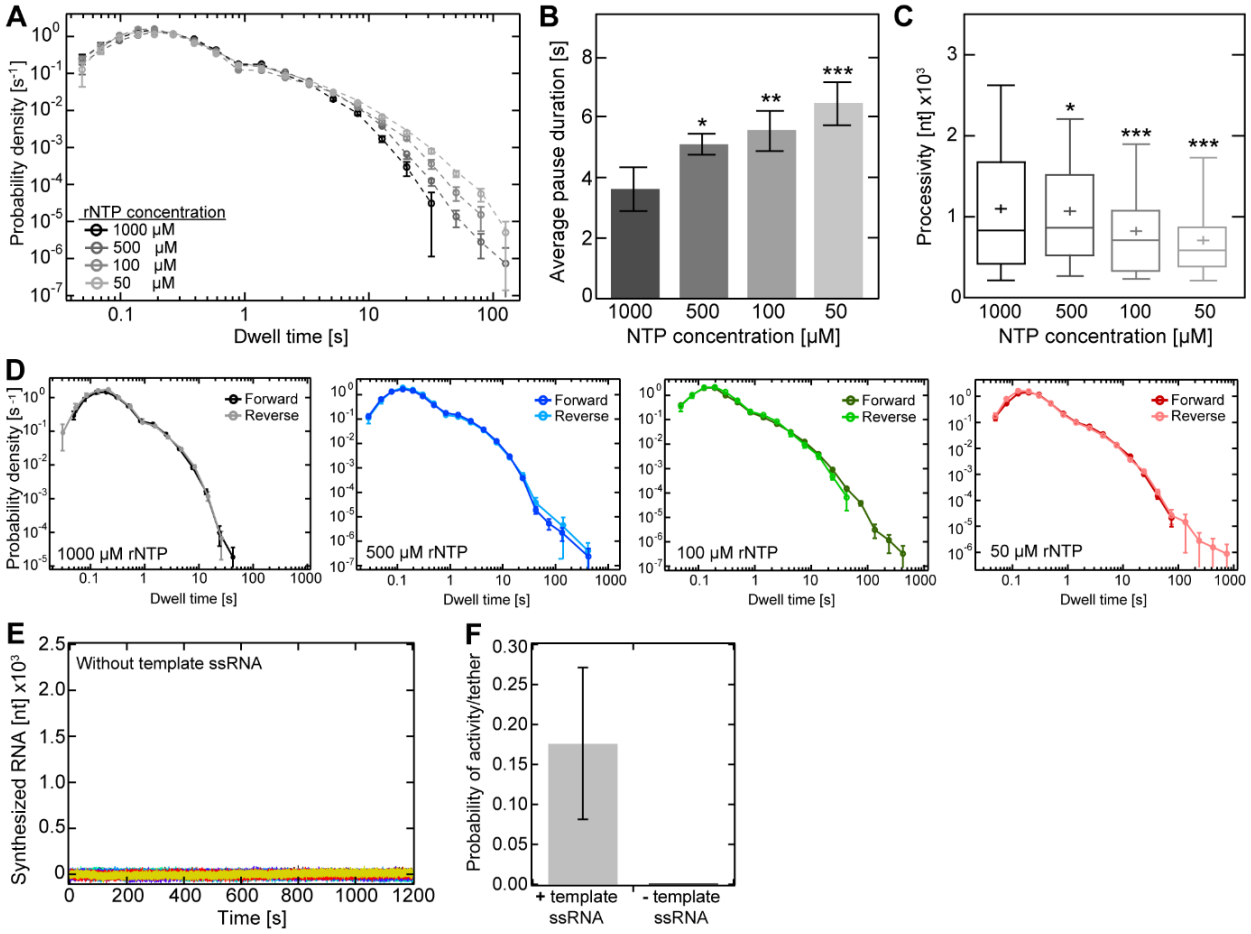

Figure S1. EV-A71 RdRp exhibits increased pausing upon nucleotides deficiency, but similar forward and reverse RNA synthesis dynamics. (**A**) Dwell time distributions of EV-A71 wild type RdRp RNA synthesis dynamics at different nucleotide concentrations (50 µM - 1 mM). Dwell time window was set to 4 nt and the error bars (±SD) result from bootstrapping with 1,000 iterations. (**B**, **C**) Comparison of extracted quantitative pause values during RNA synthesis upon nucleotide deficiency shown in **Fig. 1**, such as (**B**) average (±SEM) pause duration, and (**C**) RNA synthesis processivity. (**D**) Superimposed dwell time distributions of forward (dark colors) and reverse RNA chain elongation (light colors) at different rNTP concentrations (50 µM - 1 mM). (**E**) EV-A71 RdRp trajectories in absence of the template ssRNA strand exhibited no RNA synthesis activity. (**F**) Average probability (±SD) of RNA synthesis activity encountered in presence and absence of the template ssRNA strand (n = 100 tethers each). Statistical analyses were performed using one-way analysis of variance (ANOVA) with comparative Tukey post-hoc test (significance levels α: *** = 0.001; ** = 0.01; * = 0.05). **Related to Figure 1.**

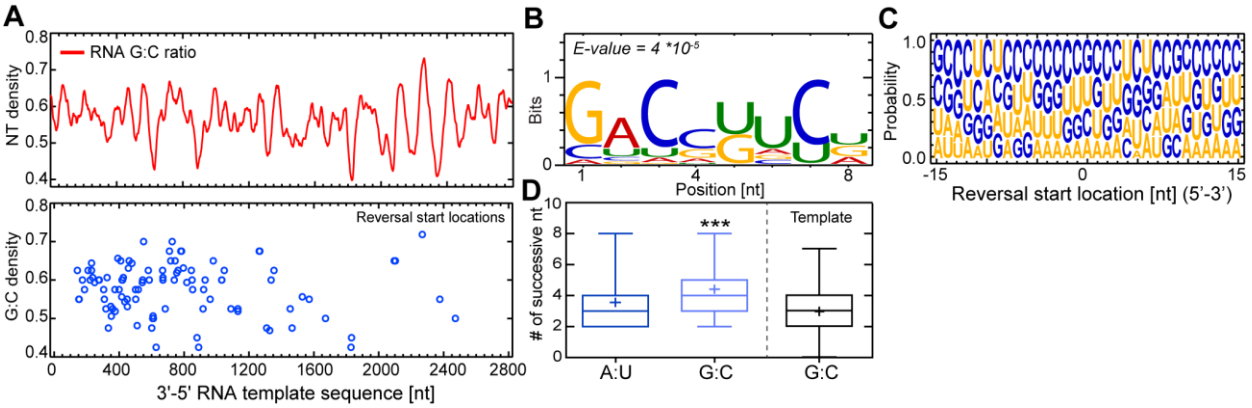

Figure S2. EV-A71 copy-back RNA synthesis occurs sequence-independent *in vitro*. (**A**) Analysis of sequences where copy-back RNA synthesis predominantly occurred (31 nt window) did not exhibit any hotspots with respect to the RNA template sequence (upper panel, red line). The G:C density at those copy-back RNA synthesis locations (lower panel, blue circles) did also not reflect any apparent correlation. (**B**) With the absence of apparent copy-back RNA synthesis hotspots, the sequences where copy-back RNA synthesis predominantly occurred were subject to *de novo* sequence motif search using MEME, a multiple sequence alignment algorithm that searches for conserved sequence motifs. The computed sequence conservation at locations of reversal events showed a bit score <1 and a probability (E-value) strongly below the 95% confidence interval threshold. Both results reveal no evidence of a predominant sequence motif as trigger. (**C**) Sequence logo of position-dependent nucleotide abundance within the sequences where copy-back RNA synthesis predominantly occurred showed that guanosines and cytosines were most abundant, which can hamper effective melting of the RNA duplex during RNA synthesis, resulting in an increase of RdRp to pause and arrest. In agreement, (**D**) a higher abundance of successive G:C (light blue) nucleotides within those sequences were found compared to both the average amount encountered in the ssRNA template (black) and successive A:U (light blue). Statistical analysis was performed using one-way analysis of variance (ANOVA) with comparative Tukey post-hoc test (significance level α: *** = 0.001). **Related to Figure 1.**

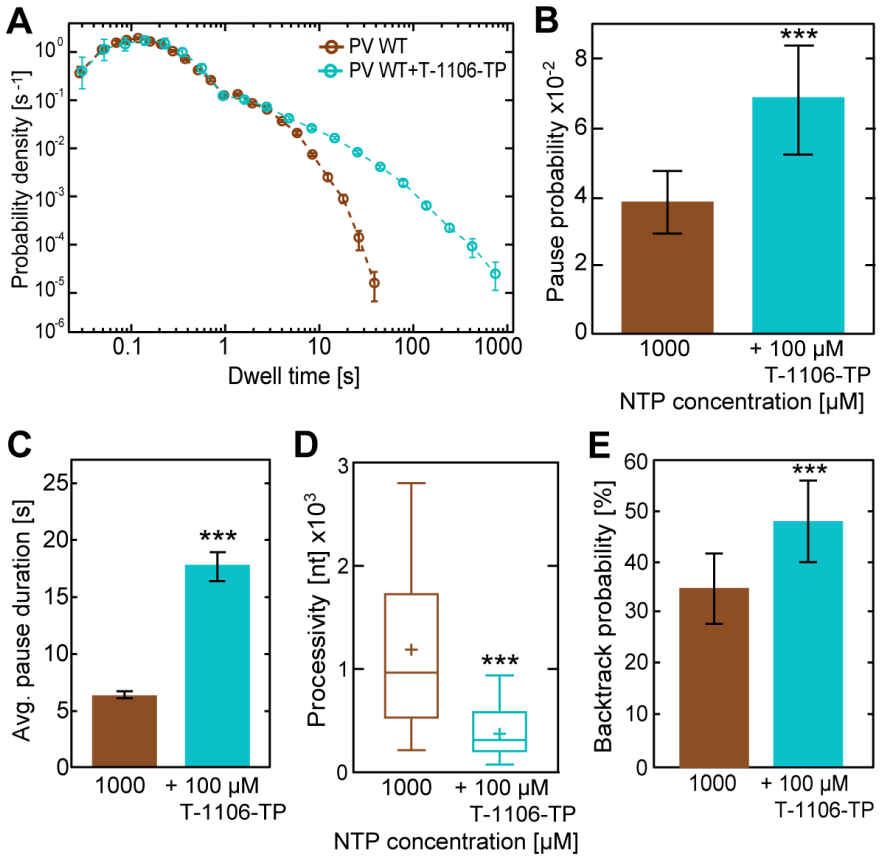

Figure S3. T-1106 increases PV RdRp pausing and backtracking. (**A**) Superimposed dwell time distributions of PV WT RdRp (brown) exhibit increased pausing probability and duration in presence of T-1160-TP (cyan). Dwell times are associated with polymerases advancing 4 nt. The error bars represent the estimate of the standard deviations via bootstrapping with 1,000 iterations. (**B-E**) In presence of T-1106-TP, wild type poliovirus RdRp exhibits significantly higher (**B**) average (±SD) pausing probability of (**C**) extended apparent duration (AVG ±SEM) during RNA synthesis, leading to a decreased (**D**) processivity but higher (**E**) backtracking probability. Statistical analysis consisted of unpaired, two-tailed t-tests (significance level p: *** ≤ 0.001; * ≤ 0.05). **Related to Figure 6.**

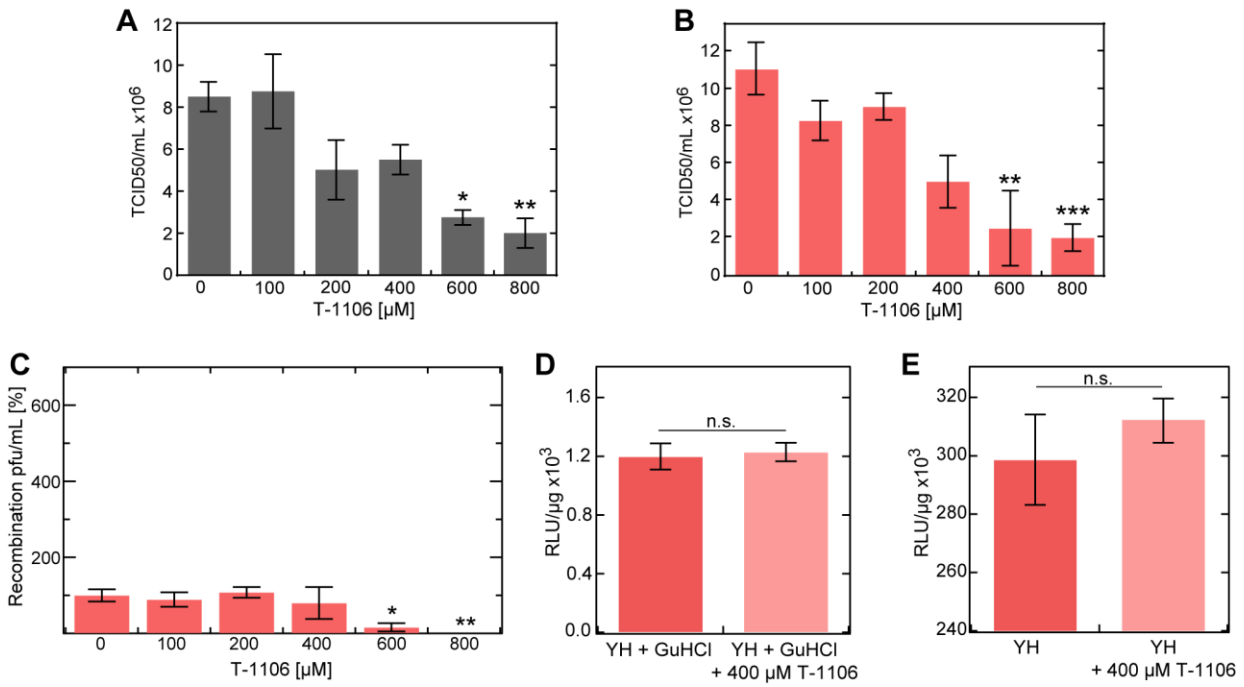

Figure S4. T-1106 dose response of EV-A71 WT and Y276H variant full-length viruses. RD cells infected with (**A**) EV-A71 wild type and (**B**) Y276H donor genomes at MOI 1 in the presence of increasing concentration of T-1106. Following total cytopathic effect (CPE), cell culture supernatants were used to quantify virus by $TCID_{50}$. (**C**) Relative Y276H viable recombinant yield normalized as a percentage of a carrier (DMSO)-treated control (AVG ±SD; n = 3 for each condition). Calculated IC_{50} amounts to 280±90 μM T-1106 (**D**, **E**) EV-A71 donor translation (**D**) and replication (**E**) efficiency (AVG ±SD) for Y276H RdRp variant. All statistical analyses were performed using one-way analyses of variance (ANOVA) with comparative Tukey post-hoc test (significance levels α: *** = 0.001; ** = 0.01; * = 0.05; n.s. = non-significant). **Related to Figure 6.**

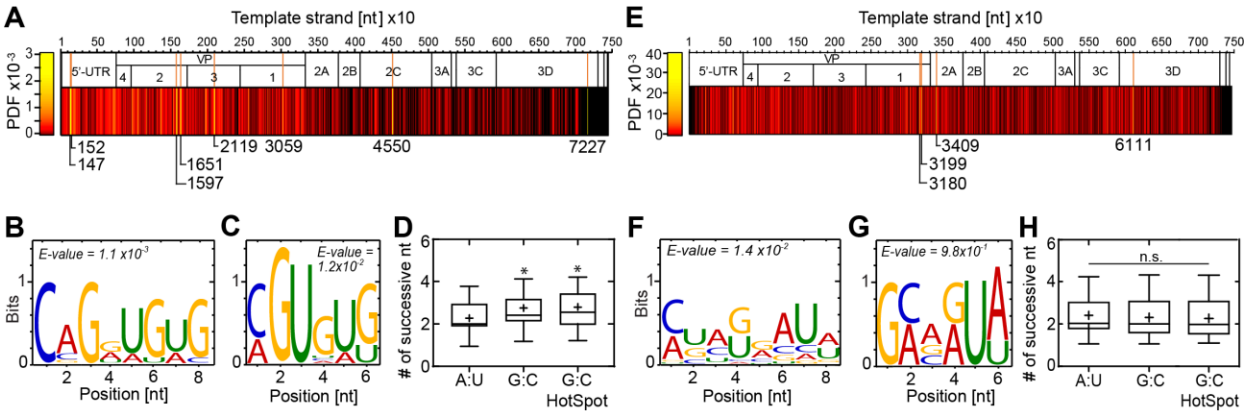

Figure S5. EV-A71 copy-back RNA synthesis and intermolecular template switching occur sequence-independent in cell culture. (**A**) Probability density plot of identified copy-back locations relative to the EV-A71 WT genome sequence. While the majority of copy-back RNA synthesis locations are randomly distributed across the genome sequence, 8 hot spots were identified at the 5'-UTR, VP2, VP3, VP1, 2C and 3D coding regions. (**B, C**) Sequences (25-nt window) where copy-back RNA synthesis occurred were subject to *de novo* sequence motif search using MEME. The computed sequence conservations for (**B**) all copy-back locations and at (**C**) copy-back hot spots reveal no evidence of a predominant or conserved sequence motif as trigger. (**D**) A higher abundance of successive G:C base pairs within the copy-back sequences were found compared to the amount of successive A:U. (**E**) Probability density plot of identified intermolecular recombination locations relative to the EV-A71 WT genome sequence. Recombination locations are randomly distributed across the genome sequence, and 4 hot spots were identified at the VP1, 2A and 3D coding regions. (**F, G**) Sequences (25-nt window) where template switching occurred were subject to *de novo* sequence motif search. The computed sequence conservations for (**F**) all recombination events and at (**G**) recombination hot spots showed also no evidence of a predominant or conserved sequence motif as trigger. (**H**) No differences in the amount of successive G:C and A:U base pairs at recombination locations and hot spots were observable. Statistical analyses were performed using one-way analysis of variance (ANOVA) with comparative Tukey post-hoc test (significance level p: * = 0.05; n.s. = non-significant). **Related to Figure 6.**

SUPPLEMENTAL TABLES

Table S1: Single molecule experimental parameters and measurement statistics. Table of experimental parameters, such as NTP and T-1106 concentrations, as well as dwell times as statistical measure for all experiments performed in this study. The number of nucleotides is an alternative statistical measure that reflects the total length of synthesized RNA monitored from pooled trajectories. The applied force was hold constant at 25 pN for all experiments. **Related to Figures 1, 3, 4, and 6.**

RdRp	**EV-A71 C2-MP4**				
[NTP]	1 mM	500 µM	100 µM	50 µM	100 µM
[NA]	-	-	-	-	50 µM T-1106
Dwell times	**9981**	**16356**	**13430**	**10042**	**6570**
Nucleotides	39.9 kb	65.4 kb	53.7 kb	40.1 kb	26.3 kb
RdRp	**EV-A71 Y276H**	**PV WT**	**PV WT**	**PV Y275H**	
[NTP]	1 mM	1 mM	1 mM	1 mM	
[NA]	-	-	100 µM T-1106	-	
Dwell times	**4881**	**5715**	**4839**	**3836**	
Nucleotides	19.5 kb	22.9 kb	19.4 kb	15.3 kb	